# Kinetic analysis of the sideband instability in a helical wiggler free-electron laser for electrons trapped near the bottom of the ponderomotive potential

Ronald C. Davidson and Jonathan S. Wurtele
*Plasma Fusion Center, Massachusetts Institute of Technology, Cambridge, Massachusetts 02139*

Richard E. Aamodt
*Science Applications International Corporation, Boulder, Colorado 80302*
(Received 6 March 1986)

A kinetic formalism based on the Vlasov-Maxwell equations is used to investigate properties of the sideband instability for a tenuous, relativistic electron beam propagating through a constant-amplitude helical wiggler magnetic field (wavelength $\lambda_0=2\pi/k_0$ and normalized amplitude $a_w=e\hat{B}_w/mc^2k_0$). The analysis is carried out for perturbations about an equilibrium Bernstein-Greene-Kruskal state in which the distribution of beam electrons $G_s(\gamma')$ and the wiggler magnetic field coexist in quasisteady equilibrium with a finite-amplitude, circularly polarized, primary electromagnetic wave $(\omega_s,k_s)$ with normalized amplitude $a_s=e\hat{B}_s/mc^2k_s$ and constant equilibrium wave phase. Particular emphasis is placed on calculating detailed properties of the sideband instability for the case where a uniform distribution of trapped electrons $G_s^T(\gamma')$ is localized near the bottom of the ponderomotive potential moving with velocity $v_p=\omega_s/(k_s+k_0)$ relative to the laboratory frame. For harmonic numbers $n\geq 2$, it is found that stable ($\mathrm{Im}\omega=0$) sideband oscillations exist for $[\omega-(k+k_0)v_p]^2\approx n^2\Omega_B^2$. Here, $(\omega,k)$ are the perturbation frequency and wave number in the laboratory frame, $\Omega_B=[a_wa_sc^2(k_p')^2/(\hat{\gamma}_M'\gamma_p)^2]^{1/2}$ is the bounce frequency, $\hat{\gamma}_M'mc^2$ is the maximum energy of the trapped electrons in the ponderomotive frame, and $k_p'$ and $\gamma_p$ are defined by $k_p'=(k_s+k_0)/\gamma_p$ and $\gamma_p=(1-v_p^2/c^2)^{-1/2}$. On the other hand, for the fundamental ($n=1$) mode, instability exists ($\mathrm{Im}\omega>0$) over a wide range of system parameters $\Omega_B/ck_0\ll 1$ and $\Gamma_0\ll 1$, where $\Gamma_0^3=(a_w^2/4)(\hat{\omega}_{pT}^2/\gamma_p^2c^2k_0^2)(1+v_p/c)[c/v_p(\hat{\gamma}_M')^3]$ and $\hat{\omega}_{pT}=(4\pi\hat{n}_Te^2/m)^{1/2}$ is the plasma frequency of the trapped electrons. Moreover, the maximum growth rate and bandwidth of the sideband instability for the fundamental ($n=1$) mode exhibit a sensitive dependence on the normalized pump strength $\Omega_B/\Gamma_0k_0c$.

## I. INTRODUCTION AND SUMMARY

Free-electron lasers,[1-4] as evidenced by the growing experimental[5-19] and theoretical[20-52] literature on this subject, can be effective sources for the generation of coherent radiation by intense electron beams. Recent experimental investigations[15-19] have been very successful over a wide range of beam energy and current ranging from experiments at low energy (150–250 keV) and low current (5–45 A),[19] to moderate energy (3.4 MeV) and high current (0.5 kA),[17,18] to high energy (20 MeV) and low current (40 A).[15,16] Theoretical studies have included investigations of nonlinear effects[20-32] and saturation mechanisms, the influence of finite geometry on linear stability properties,[33-38] novel magnetic field geometries for radiation generation,[38-43] and fundamental studies of stability behavior.[44-52] In a recent calculation,[32] a self-consistent kinetic formalism has been developed to describe the sideband instability[24] within the framework of the Vlasov-Maxwell equations for a relativistic electron beam propagating through a helical wiggler magnetic field. Unlike previous studies of the sideband instability, the analysis[32] is carried out for perturbations about an equilibrium Bernstein-Greene-Kruskal (BGK) state[29] in which the beam electrons, the wiggler magnetic field, and a finite-amplitude primary electromagnetic wave $(\omega_s,k_s)$ coexist in quasisteady equilibrium. In the present analysis, we make use of the general kinetic formalism developed in Ref. 32 to carry out a detailed investigation of the sideband instability for the case where the trapped electrons are localized near the bottom of the ponderomotive potential.

The theoretical model[32] and assumptions are reviewed briefly in Sec. II. The relativistic electron beam has uniform cross section and propagates in the $z$ direction through the constant-amplitude helical magnetic wiggler field [Eq. (1)] with wavelength $\lambda_0=2\pi/k_0$ and normalized amplitude $a_w=e\hat{B}_w/mc^2k_0$. The theoretical model neglects longitudinal perturbations ($\delta\phi\simeq 0$) and transverse spatial variations ($\partial/\partial x=0=\partial/\partial y$), and beam distribution functions

$$f_b(z,\mathbf{p},t)=\hat{n}_b\delta(P_x)\delta(P_y)G(z,p_z,t)$$

with zero transverse canonical momenta are considered [Eq. (4)]. Moreover, the stability analysis is carried out for perturbations about an equilibrium BGK state in which the distribution of beam electrons $G_s(\gamma')$ and the

 

wiggler magnetic field [Eq. (1)] coexist in quasisteady equilibrium[29] with a constant-amplitude, circularly polarized, primary electromagnetic wave $(\omega_s,k_s)$ with normalized amplitude $a_s=e\hat{B}_s/mc^2k_s$ and constant equilibrium wave phase [Eqs. (2) and (3)]. Transforming the linearized Vlasov-Maxwell equations to the ponderomotive frame moving with velocity $v_p=\omega_s/(k_s+k_0)$ leads to the formal dispersion relation (8) in the diagonal approximation. Here, the trapped- and untrapped-electron susceptibilities, $\chi_0^T(k',\omega')$ and $\chi_0^U(k',\omega')$, are defined in Eqs. (10) and (14) in terms of the exact electron trajectories in the ponderomotive frame including the full influence of the finite-amplitude primary electromagnetic wave $(\omega_s,k_s)$.

Detailed properties of the sideband instability are investigated in Sec. III for the case where the trapped electrons are localized near the bottom of the ponderomotive potential [Eq. (18)]. Assuming wave perturbations with (nearly) right-circular polarization, and neglecting the contribution of the untrapped electrons, the dispersion relation can be expressed as [Eq. (25)]

$$\omega^2-c^2k^2-\hat{\alpha}_0\hat{\omega}_{pb}^2=-a_w^2\hat{\omega}_{pT}^2\sum_{n=1}^{\infty}\int_{\hat{\gamma}'_-}^{\hat{\gamma}'_+}\frac{d\gamma'}{\gamma'}\frac{\partial\hat{G}_s^T}{\partial\gamma'}\frac{n^2\hat{\omega}_B^2(\gamma')J_n^2[k'_Lz'_T(\gamma')]}{\gamma_p^2[\omega-(k+k_0)v_p]^2-n^2\hat{\omega}_B^2(\gamma')}\ ,$$

where $\hat{G}_s^T(\gamma')$ is the (normalized) distribution of trapped electrons,

$$\gamma'mc^2=[1+(p'_z)^2/m^2c^2+a_w^2+a_s^2-2a_wa_s\cos(k'_pz')]^{1/2}mc^2$$

is the electron energy in the ponderomotive frame, and $(\omega,k)$ denotes the perturbation frequency and wave number in the laboratory frame. To summarize the other pertinent definitions in Eq. (25), we note that

$$k'_L=\gamma_p(k+k_0-v_p\omega/c^2),\quad k'_p=(k_s+k_0)/\gamma_p\ ,$$
$$v_p=\omega_s/(k_s+k_0),\quad \gamma_p=(1-v_p^2/c^2)^{-1/2}\ .$$

Moreover,

$$\hat{\omega}_B(\gamma')=(a_wa_sc^2k_p'^2/\gamma'^2)^{1/2}$$

is the bounce frequency of electrons trapped near the bottom of the ponderomotive potential, $\hat{\alpha}_0$ is a constant of order unity,[32] $\omega_{pb}^2=4\pi\hat{n}_be^2/m$ is the plasma frequency squared of the beam electrons, $\hat{\omega}_{pT}^2=4\pi\hat{n}_Te^2/m$ is the plasma frequency squared of the trapped electrons, $\hat{n}_T$ is the (average) density of the trapped electrons, the orbital turning points $\pm z_T(\gamma')$ are determined from

$$k_p'^2z_T'^2(\gamma')=(\gamma'^2-\hat{\gamma}'^2_{\mp})/a_wa_s\ ,$$

and $\hat{\gamma}'_+$ and $\hat{\gamma}'_-$ are defined by

$$\hat{\gamma}'_{\pm}=[1+(a_w\pm a_s)^2]^{1/2}\ .$$

In circumstances where the trapped electrons are localized near the bottom of the ponderomotive potential, the stability properties calculated from Eq. (25) are relatively insensitive[32] to the detailed form of $\hat{G}_s^T(\gamma')$. Therefore, in Sec. III A, we consider the case where the trapped electrons are uniformly distributed in $\gamma'$ from $\gamma'=\hat{\gamma}'_-$ to $\gamma'=\hat{\gamma}'_M$ [Eq. (27)], where $(\hat{\gamma}'_M)^2-(\hat{\gamma}'_-)^2\ll(\hat{\gamma}'_+)^2-(\hat{\gamma}'_-)^2=4a_wa_s$ for electrons trapped near the bottom of the ponderomotive potential. For the choice of distribution function in Eq. (27), the dispersion relation can be expressed as [Eq. (28)]

$$\omega^2-c^2k^2-\hat{\alpha}_0\hat{\omega}_{pb}^2=a_w^2\hat{\omega}_{pT}^2\sum_{n=1}^{\infty}\frac{n^2\Omega_B^2C_n(k,\omega)}{[\omega-(k+k_0)v_p]^2-n^2\Omega_B^2}\ ,$$

where

$$\Omega_B=\hat{\omega}_B(\gamma'=\hat{\gamma}'_M)/\gamma_p=[a_wa_sc^2(k'_p)^2/(\hat{\gamma}'_M)^2\gamma_p^2]^{1/2}\ ,$$

and the $n$th harmonic coupling coefficient $C_n(k,\omega)$ is defined in Eq. (29). An examination of Eq. (29) for $(k'_L)^2z_T'^2(\gamma'=\hat{\gamma}'_M)/4\ll1$ shows that the harmonic contributions in Eq. (28) decrease rapidly with increasing $n$ for $n\geq2$. Moreover, it is found that the harmonic contributions in Eq. (28) for $n\geq2$ lead to *stable* oscillations with $\mathrm{Im}\omega=0$.

In Secs. III B and III C, we investigate properties of the sideband instability for the fundamental $(n=1)$ mode. Neglecting the harmonic contributions in Eq. (28) for $n\geq2$ leads to the dispersion relation (39), which can be approximated by [Eq. (42)]

$$[(\delta\omega-v_p\delta k)^2-\Omega_B^2]\left[(\delta\omega-v_p\delta k)-ck_0\frac{v_p}{c}\left[\frac{\delta k}{\hat{k}_c}+\epsilon_b\right]\right]=\Gamma_0^3c^3k_0^3\ .$$

Here, $\delta\omega=\omega-\hat{\omega}_c$ and $\delta k=k-\hat{k}_c$, where

$$\hat{k}_c=\gamma_p^2(1+v_p/c)(v_p/c)k_0$$

and $\hat{\omega}_c=c\hat{k}_c$ are the upshifted wave number and frequency. Moreover, the small parameter

$$\epsilon_b=(\hat{\alpha}_0\hat{\omega}_{pb}^2/2\gamma_p^2k_0^2v_p^2)(1+v_p/c)^{-1}\ll1$$

describes the (small) shift in wave number and frequency produced by beam dielectric effects. Finally,

$$\Omega_B/ck_0=[(a_wa_s)^{1/2}/\hat{\gamma}'_M](1+v_p/c)\ll1$$

for $a_s\ll1$ and $\omega_s\simeq ck_s$, and the small dimensionless parameter $\Gamma_0^3$ is defined by [Eq. (45)]

$$\Gamma_0^3=\frac{1}{4}\frac{a_w^2}{(1+a_w^2)^{3/2}}\frac{\hat{\omega}_{pT}^2}{\gamma_p^2c^2k_0^2}\frac{(1+v_p/c)}{v_p/c}\ll 1 .$$

Equation (42) is a cubic equation which determines the complex oscillation frequency $(\delta\omega-v_p\delta k)$ in terms of $\delta k/\hat{k}_c$ and the dimensionless parameters $\Gamma_0$, $\Omega_B/ck_0$, and $\epsilon_b$. A detailed analysis of Eq. (42) [or equivalently, Eqs. (44) or (48)] is presented in Sec. III C. As a general remark, for $\Gamma_0\ll 1$, it is found that the *lower* sideband exhibits instability ($\mathrm{Im}\delta\omega>0$) for $\delta\omega$ and $\delta k$ in the vicinity of the simultaneous resonance conditions

$$\delta\omega-v_p\delta k=-\Omega_B ,$$

$$\delta\omega-v_p\delta k=ck_0\frac{v_p}{c}\left[\frac{\delta k}{\hat{k}_c}+\epsilon_b\right] .$$

Denoting the simultaneous solutions to these equations by $(\delta\hat{\omega},\delta\hat{k})$, we obtain for the central wave number $\hat{k}=\hat{k}_c+\delta\hat{k}$ and frequency $\hat{\omega}=\hat{\omega}_c+\delta\hat{\omega}$ of the lower sideband [Eq. (35)]

$$\hat{k}=\gamma_p^2\left[1+\frac{v_p}{c}\right]\frac{v_p}{c}k_0\left[1-\epsilon_b-\frac{\Omega_B}{k_0v_p}\right] ,$$

$$\hat{\omega}=\gamma_p^2\left[1+\frac{v_p}{c}\right]k_0v_p\left[1-\epsilon_b\frac{v_p}{c}-\frac{\Omega_B}{k_0v_p}\right] ,$$

where

$$\hat{k}_c=\gamma_p^2(1+v_p/c)(v_p/c)k_0 .$$

Moreover, it is found that the corresponding growth rate $\mathrm{Im}(\delta\omega)$ and instability bandwidth (in $\delta k$ space) exhibit a sensitive dependence on the normalized pump strength $\Omega_B/\Gamma_0k_0c$. For example, for $k=\hat{k}_c+\delta\hat{k}=\hat{k}$, the characteristic maximum growth rate $\mathrm{Im}(\delta\omega)$ calculated from Eq. (42) is given by [Eq. (49)]

$$\mathrm{Im}(\delta\omega)=\Gamma_0k_0c\frac{(3)^{1/2}}{(2)^{5/3}}\left[1+\frac{32}{27}\frac{\Omega_B^3}{\Gamma_0^3k_0^3c^3}\right]^{1/3}\times\left\{\left[1+\left[1+\frac{32}{27}\frac{\Omega_B^3}{\Gamma_0^3k_0^3c^3}\right]^{-1/2}\right]^{2/3}-\left[1-\left[1+\frac{32}{27}\frac{\Omega_B^3}{\Gamma_0^3k_0^3c^3}\right]^{-1/2}\right]^{2/3}\right\} .$$

In the weak-pump regime ($\Omega_B/\Gamma_0k_0c\ll 1$), the instability is relatively broadband, and the characteristic maximum growth rate is [Eq. (50)]

$$\mathrm{Im}(\delta\omega)=\frac{(3)^{1/2}}{2}\Gamma_0k_0c .$$

On the other hand, in the strong-pump regime ($\Omega_B/\Gamma_0k_0c\gg 1$), the characteristic maximum growth rate is [Eq. (51)]

$$\mathrm{Im}(\delta\omega)=\frac{\Gamma_0k_0c}{(2)^{1/2}}\left[\frac{\Gamma_0k_0c}{\Omega_B}\right]^{1/2} ,$$

and the corresponding (narrow) bandwidth is given by [Eq. (56)]

$$\frac{\Delta k}{\hat{k}_c}=2\Gamma_0\frac{c}{v_p}\left[\frac{2\Gamma_0k_0c}{\Omega_B}\right]^{1/2} .$$

From Eqs. (50), (51), and (56), we note that the growth rate and bandwidth of the sideband instability are greatly reduced as the dimensionless pump strength is increased to the regime where $\Omega_B/\Gamma_0k_0c\gg 1$.

As a final point, the dispersion relation (25) and related analysis in Sec. III are valid for electromagnetic wave perturbations with *right-circular* polarization, in which case it is found that only the *lower* sideband exhibits instability. A completely parallel analysis can be carried out in circumstances where the wave perturbations have *left-circular* polarization.[32] In this case, it is found[32] that the role of the lower and the upper sidebands is reversed, and the *upper* sideband exhibits instability for perturbations with left-circular polarization.

## II. KINETIC DISPERSION RELATION

The present analysis assumes a relativistic electron beam with uniform cross section propagating in the $z$ direction through the constant-amplitude helical wiggler magnetic field $\mathbf{B}_w(\mathbf{x})=\nabla\times\mathbf{A}_w(\mathbf{x})$ with vector potential

$$\mathbf{A}_w(\mathbf{x})=-\frac{\hat{B}_w}{k_0}[\cos(k_0z)\hat{\mathbf{e}}_x+\sin(k_0z)\hat{\mathbf{e}}_y] . \tag{1}$$

Here, $\lambda_0=2\pi/k_0=\mathrm{const}$ is the wavelength, and $\hat{B}_w=\mathrm{const}$ is the amplitude of the wiggler magnetic field. It is assumed that the electron beam is sufficiently tenuous that the Compton-regime approximation is valid with negligibly small longitudinal fields ($\delta\phi\simeq 0$). Moreover, the beam density and current are assumed to be sufficiently small that the influence of equilibrium self-electric and self-magnetic fields on the particle trajectories and stability behavior can be neglected. That is, the present analysis neglects the effects of the self-electric field and the self-magnetic field associated with the equilibrium space charge and axial current, respectively, of the electron beam. For purposes of investigating the sideband instability, it is also assumed that perturbations are about a circularly polarized, constant-amplitude, monochromatic, electromagnetic wave $(\omega_s,k_s)$ with vector potential

$$\mathbf{A}_s(\mathbf{x},t)=\frac{\hat{B}_s}{k_s}[\cos(k_sz-\omega_st)\hat{\mathbf{e}}_x-\sin(k_sz-\omega_st)\hat{\mathbf{e}}_y] , \tag{2}$$

and electric and magnetic fields given by

$$\mathbf{E}_s(\mathbf{x},t)=-\frac{1}{c}\frac{\partial}{\partial t}\mathbf{A}_s(\mathbf{x},t)\ ,$$
$$\mathbf{B}_s(\mathbf{x},t)=\nabla\times\mathbf{A}_s(\mathbf{x},t)\ . \tag{3}$$

Here, $\hat{B}_s=$const is the magnetic field amplitude of the electromagnetic wave. The electromagnetic wave described by Eqs. (2) and (3) should be viewed as the primary free-electron-laser (FEL) signal that develops after a period of linear growth and saturation. The present analysis assumes that the distribution of beam electrons, the wiggler field [Eq. (1)], and the primary electromagnetic wave field [Eqs. (2) and (3)] coexist in a quasisteady equilibrium BGK state.[29] Moreover, we examine the class of exact solutions to the fully nonlinear Vlasov equation of the form[47,48]

$$f_b(z,\mathbf{p},t)=\hat{n}_b\delta(P_x)\delta(P_y)G(z,p_z,t)\ , \tag{4}$$

where $\hat{n}_b=$const is the density, and

$$P_x=p_x-(e/c)A_{xw}(z)-(e/c)A_{xs}(z,t)-(e/c)\delta A_x(z,t)$$

and

$$P_y=p_y-(e/c)A_{yw}(z)-(e/c)A_{ys}(z,t)-(e/c)\delta A_y(z,t)$$

are the transverse canonical momenta. Within the context of the assumptions in the present analysis, we note that $P_x$ and $P_y$ are exact single-particle constants of the motion. Moreover, the class of distribution functions with $P_x=0=P_y$ in Eq. (4) corresponds to an "ideal" electron beam with zero transverse emittance. The Vlasov-Maxwell equations[32] are then linearized for small-amplitude perturbations about the equilibrium BGK state[29] characterized by the wiggler magnetic field (normalized amplitude $=a_w=e\hat{B}_w/mc^2k_0$), the primary electromagnetic wave $(\omega_s,k_s)$ (normalized amplitude $=a_s=e\hat{B}_s/mc^2k_s$), and the corresponding self-consistent distribution of beam electrons $G_s(\gamma')$. Here,

$$\gamma' mc^2=[1+(p_z')^2/m^2c^2+a_w^2+a_s^2-2a_wa_s\cos(k_p'z')]^{1/2}mc^2$$

is the electron energy in the *ponderomotive frame* moving with axial velocity

$$v_p=\frac{\omega_s}{k_s+k_0}\ , \tag{5}$$

and $k_p'$ is defined by $k_p'=(k_s+k_0)/\gamma_p$, where $\gamma_p=(1-v_p^2/c^2)^{-1/2}$. In the absence of wave perturbations $(\delta A_x=0=\delta A_y)$ about the electromagnetic field configuration described by Eqs. (1)–(3), it should be noted that the energy $\gamma' mc^2$ in the ponderomotive frame [defined prior to Eq. (5)] is an exact constant of the motion. Therefore, in ponderomotive frame variables, the corresponding distribution function

$$f_b=\hat{n}_b\delta(P_x')\delta(P_y')G_s(\gamma')$$

is an exact equilibrium solution[29,32] to the fully nonlinear Vlasov equation.

It should be emphasized that to maintain a primary electromagnetic wave with constant amplitude and constant phase [$\delta_s=0$ in Eq. (2)] necessarily requires both untrapped- and trapped-electron populations.[29,32] Indeed, the Maxwell equations for $\mathbf{A}_s(\mathbf{x},t)$ can be used to derive an integral equation which expresses the distribution of trapped electrons $G_s^T(\gamma')$ directly in terms of the distribution of untrapped electrons $G_s^U(\gamma')$ [Eq. (48) of Ref. 29].

To summarize briefly, the linearized Vlasov-Maxwell equations are transformed to the ponderomotive frame, where it is found that the linearized equations for the perturbed distribution function $\delta G(z',p_z',t')$ and the normalized vector potential

$$\delta A^{\pm}(z',t')\equiv(e/mc^2)\exp(\mp ik_0z')[\delta A_x(z',t')\pm i\delta A_y(z',t')]$$

assume particularly simple forms. In the ponderomotive frame ("primed" variables), the linearized Vlasov-Maxwell equations are combined to give the eigenvalue equation[32]

$$\left[(\omega')^2+c^2\frac{\partial^2}{\partial z'^2}-c^2k_0^2\pm 2ik_0c^2\gamma_p\left(\frac{\partial}{\partial z'}+\frac{i\omega' v_p}{c^2}\right)-\alpha_1\hat{\omega}_{pb}^2\right]\delta\hat{A}^{\pm}(z')$$
$$=-\alpha_3\hat{\omega}_{pb}^2[\delta\hat{A}^{+}(z')+\delta\hat{A}^{-}(z')]+\tfrac{1}{2}i\omega' a_w^2\hat{\omega}_{pb}^2\int\frac{dp_z'}{(\gamma')^2}\frac{\partial G_s}{\partial\gamma'}\int_{-\infty}^{t'}dt''\exp[-i\omega'(t''-t')]$$
$$\times[\delta\hat{A}^{+}(z''(t''))+\delta\hat{A}^{-}(z''(t''))] \tag{6}$$

for the potential amplitude $\delta\hat{A}^{\pm}(z')$ and the complex oscillation frequency $\omega'$. Here, an FEL oscillator is assumed, with $\mathrm{Im}\omega'>0$ corresponding to temporal growth. Moreover, $G_s(\gamma')$ is the equilibrium distribution function in the ponderomotive frame, $\hat{\omega}_{pb}^2=4\pi\hat{n}_be^2/m$ is the nonrelativistic plasma frequency-squared, and $\alpha_1(k_p'z')$ and $\alpha_3(k_p'z')$ are coefficients of order unity. An important feature of the eigenvalue equation (6) is that the electron orbit $z''(t'')$, which occurs in the orbit integral on the right-hand side of Eq. (6), can be calculated in closed analytical form in the ponderomotive frame from

$$(\gamma')^2\left(\frac{dz''}{dt''}\right)^2=c^2[\gamma'^2-1-a^2(z'')] \tag{7}$$

for both the trapped and untrapped electrons. In Eq. (7), $\gamma' mc^2 = \text{const}$ is the electron energy in the ponderomotive frame, and $a^2(z'')$ is defined by

$$a^2(z'') = a_w^2 + a_s^2 - 2a_w a_s \cos(k_p' z'') \ .$$

Equation (7) is to be solved for $z''(t'')$ subject to the boundary conditions $z''(t''=t')=z'$ and $p_z''(t''=t')=p_z'$.

A Fourier decomposition of the $z'$ dependence of the eigenvalue equation (6) leads to a matrix dispersion equation relating the Fourier components of the perturbed vector potential. In the *diagonal approximation,* we neglect the coupling of wave component $k'$ to $k' \pm s k_p'$ ($s=1,2,\ldots$). For electromagnetic perturbations with nearly right-circular polarization, we obtain the diagonal dispersion relation[32]

$$D_T(k',\omega') = -[\chi_0^T(k',\omega') + \chi_0^u(k',\omega')] \ , \tag{8}$$

where $D_T(k',\omega')$ is defined by

$$D_T(k',\omega') = (\omega')^2 - c^2(k'^2 + k_0^2 - 2k_0 k' \gamma_p - 2k_0 \omega' \gamma_p v_p / c^2) - \alpha_0 \hat{\omega}_{pb}^2 \ , \tag{9}$$

and $\alpha_0$ is a constant coefficient of order unity. In the dispersion relation (8), using techniques similar to those developed by Goldman[53,54] for electrostatic trapped-particle instabilities in nonrelativistic plasma, the *trapped-electron susceptibility* $\chi_0^T(k',\omega')$ can be expressed in the classic form of a sum over oscillators[32]

$$\chi_0^T(k',\omega') = -\tfrac{1}{2} a_w^2 \hat{\omega}_{pb}^2 \sum_{n=-\infty}^{\infty} \int_{\hat{\gamma}'_-}^{\hat{\gamma}'_+} d\gamma' \frac{F_n^T(\gamma')}{(\omega')^2 - n^2 \omega_B^2(\gamma')} \ , \tag{10}$$

where the oscillator strength $F_n^T(\gamma')$ is defined by

$$F_n^T(\gamma') = -\omega'^2 \frac{mc}{\gamma'} \frac{\partial G_s^T}{\partial \gamma'} \times \int_{-z_T'(\gamma')}^{z_T'(\gamma')} \frac{dz'}{\lambda_p'} \frac{a_n^T(z',\gamma')}{[(\gamma')^2 - 1 - a^2(z')]^{1/2}} \ . \tag{11}$$

Here, the coefficient $a_n^T(z',\gamma')$ is defined by

$$a_n^T(z',\gamma') = \frac{1}{\tau_B(\gamma')} \int_0^{\tau_B(\gamma')} d\tau \exp\{ik'[z''(\tau) - z'] - in\omega_B(\gamma')\tau\} \ , \tag{12}$$

where $\tau = t'' - t'$,

$$\omega_B(\gamma') = \pi \hat{\omega}_B(\gamma') / 2F(\pi/2, \kappa_T)$$

is the bounce frequency of a trapped electron with energy $\gamma' mc^2$, $\tau_B(\gamma') = 2\pi/\omega_B(\gamma')$ is the bounce period, $F(\eta,\kappa_T)$ is the elliptic integral of the first kind,

$$\hat{\omega}_B(\gamma') = [a_w a_s c^2 (k_p')^2 / \gamma'^2]^{1/2}$$

is the bounce frequency near the bottom of the ponderomotive potential, $\kappa_T$ is defined by

$$\kappa_T^2 = [(\gamma')^2 - (\hat{\gamma}'_-)^2] / 4a_w a_s \ ,$$

and $\lambda_p' = 2\pi/k_p'$ is the wavelength of the ponderomotive potential. In Eq. (11), $G_s^T(\gamma')$ is the energy distribution of the trapped electrons, and the orbital turning points $\pm z_T'(\gamma')$ are determined from[32]

$$(\gamma')^2 = (\hat{\gamma}'_-)^2 + 4a_w a_s \sin^2[k_p' z_T'(\gamma')/2] \ . \tag{13}$$

In Eqs. (10) and (13), assuming $a_w > 0$ and $a_s > 0$ without loss of generality, the quantities $\hat{\gamma}'_+$ and $\hat{\gamma}'_-$ are defined by

$$\hat{\gamma}'_\pm = [1 + (a_w \pm a_s)^2]^{1/2} \ ,$$

corresponding to the maximum ($\hat{\gamma}'_+$) and minimum ($\hat{\gamma}'_-$) allowable energy of an electron trapped in the ponderomotive potential (Fig. 1). In a similar manner, the *untrapped-electron susceptibility* $\chi_0^U(k',\omega')$ occurring in the dispersion relation (8) can be expressed as[32]

$$\chi_0^U(k',\omega') = -\tfrac{1}{2} a_w^2 \hat{\omega}_{pb}^2 \sum_{n=-\infty}^{\infty} \int_{\hat{\gamma}'_+}^{\infty} d\gamma' \left[ \frac{F_n^>(\gamma')}{[\omega' - (k' + nk_p')\beta_U'(\gamma')c]} + \frac{F_n^<(\gamma')}{[\omega' + (k' + nk_p')\beta_U'(\gamma')c]} \right] , \tag{14}$$

where $F_n^{\gtrless}(\gamma')$ is defined by

$$F_n^{\gtrless}(\gamma') = -\omega' \frac{mc}{\gamma'} \frac{\partial G_s^{\gtrless}}{\partial \gamma'} \int_{-\lambda_p'/2}^{\lambda_p'/2} \frac{dz'}{\lambda_p'} \frac{a_n^U(z',\gamma')}{[\gamma'^2 - 1 - a^2(z')]^{1/2}} \ , \tag{15}$$

and the coefficient $a_n^U(z',\gamma')$ is defined by

$$a_n^U(z',\gamma') = \frac{1}{\tau_U(\gamma')} \int_0^{\tau_U(\gamma')} d\tau \exp\{ik'[z''(\tau) - z'] - i(k' + nk_p')\beta_U'(\gamma')c\tau\} \ . \tag{16}$$

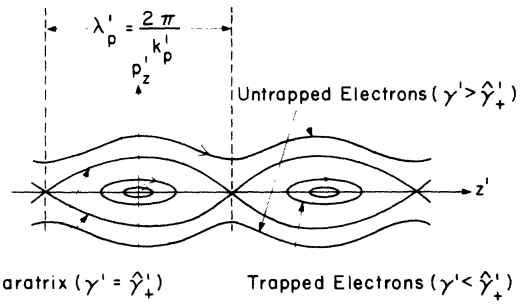


FIG. 1. In the ponderomotive frame, electron motion in the phase space $(z',p'_z)$ occurs on surfaces with $\gamma'=$const.

In Eqs. (15) and (16), $\beta'_U(\gamma')c$ is the axial velocity of an untrapped electron, $\tau_U(\gamma')$ is defined by

$$\tau_U(\gamma')=2\pi/k'_p\beta'_U(\gamma')c \ ,$$

$G_s^>(\gamma')$ is the distribution of forward-moving ($p'_z>0$) untrapped electrons, and $G_s^<(\gamma')$ is the distribution of backward-moving ($p'_z<0$) untrapped electrons in the ponderomotive frame.

The dispersion relation (8), together with the definitions of $D_T(k',\omega')$, $\chi_0^T(k',\omega')$, and $\chi_0^U(k',\omega')$ in Eqs. (9), (10), and (14), respectively, can be used to investigate detailed FEL stability properties over a wide range of system parameters. In this regard, the expressions for the trapped- and untrapped-electron susceptibilities in Eqs. (10) and (14) are valid for a broad class of BGK distribution functions $G_s(\gamma')$ which coexist in quasisteady equilibrium with the wiggler field [Eq. (1)] and the constant-amplitude primary electromagnetic wave $(\omega_s,k_s)$ [Eqs. (2) and (3)]. Note that Eqs. (10) and (14) are rich in harmonic content, with resonant behavior in the integrands occurring for $\omega'^2\approx n^2\omega_B^2(\gamma')$ for the trapped electrons, and for

$$\omega'\approx\pm(k'+nk'_p)\beta'_U(\gamma')c$$

for the untrapped electrons.

It is important to comment on a notational point. In obtaining the eigenvalue equation (6), we have introduced the normalized vector potential

$$\delta A^{\pm}(z,t)=\exp(\mp ik_0z)(e/mc^2)$$
$$\times[\delta A_s(z,t)\pm i\delta A_y(z,t)] \ ,$$

which includes the scaling factor $\exp(\mp ik_0z)$. Subsequently, in ponderomotive-frame variables, there is a Fourier decomposition of the $z'$ dependence of

$$\delta A^{\pm}(z',t')=\delta\hat{A}^{\pm}(z')\exp(-i\omega't') \ .$$

As a consequence of the scaling factor $\exp(\mp ik_0z)$, the laboratory-frame wave number should be shifted by one additional unit of $k_0$ to give the familiar condition for beam synchronism with the ponderomotive wave. In particular, for perturbations with right-circular polarization described by the dispersion relation (8), the frequency and wave number $(\omega',k')$ in the ponderomotive frame are related to the frequency and wave number $(\omega,k)$ in the laboratory frame by

$$\omega'=\gamma_p[\omega-(k+k_0)v_p] \ ,$$
$$k'=\gamma_p(k+k_0-v_p\omega/c^2) \ , \tag{17}$$

where $v_p=\omega_s/(k_s+k_0)$ and $\gamma_p=(1-v_p^2/c^2)^{-1/2}$.

## III. SIDEBAND INSTABILITY

### A. Dispersion relation for electrons trapped near the bottom of the ponderomotive potential

The formal dispersion relation (8) is a very general result which can be used to investigate detailed FEL stability properties over a wide range of system parameters, choices of distribution function $G_s(\gamma')$, and frequency regimes.[32] For present purposes, we make use of Eq. (8) to investigate the sideband instability, with particular emphasis on the case where the trapped electrons are localized near the bottom of the ponderomotive potential with

$$\frac{(k'_p)^2z_T'^2(\gamma')}{4}\ll 1 \ . \tag{18}$$

The corresponding orbit $z''(\tau)$ calculated from Eq. (7) then exhibits simple harmonic motion with frequency

$$\hat{\omega}_B(\gamma')=[a_wa_sc^2(k'_p)^2/(\gamma')^2]^{1/2} \ .$$

While this is a very restrictive assumption, the analysis gives useful physical insights as to the nature of the instability. For present purposes, we also assume that $\omega'$ is well removed from the resonances

$$\omega'\approx\pm(k'+nk'_p)\beta'_U(\gamma')c$$

characteristic of the untrapped electrons, and the term $\chi_0^U(k',\omega')$ is neglected in Eq. (8). The dispersion relation (8) can then be approximated by

$$D_T(k',\omega')=-\chi_0^T(k',\omega')$$
$$=\tfrac{1}{2}a_w^2\hat{\omega}_{pb}^2\sum_{n=-\infty}^{\infty}\int_{\hat{\gamma}'_-}^{\hat{\gamma}'_+}d\gamma'\frac{F_n^T(\gamma')}{(\omega')^2-n^2\omega_B^2(\gamma')} \ , \tag{19}$$

where the oscillator strength $F_n^T(\gamma')$ is defined in Eq. (11).

After some tedious algebraic manipulation that makes use of Eqs. (11) and (12) and the axial orbit

$$z''(\tau)=\frac{p'_z}{\gamma' m\hat{\omega}_B(\gamma')}\sin[\hat{\omega}_B(\gamma')\tau]+z'\cos[\hat{\omega}_B(\gamma')\tau] \tag{20}$$

calculated from Eq. (7) near the bottom of the ponderomotive potential, it can be shown that[32]

$$F_n^T(\gamma')+F_{-n}^T(\gamma')=-(\omega')^2\frac{mc^2k'_p}{(\gamma')^2\hat{\omega}_B(\gamma')}\frac{\partial G_s^T}{\partial\gamma'}$$
$$\times J_n^2[k'z'_T(\gamma')] \ , \tag{21}$$

where $J_n(x)$ is the Bessel function of the first kind of or-

der $n$. Here, the turning points $\pm z_T(\gamma')$ are determined from

$$(k_p')^2 z_T'^2(\gamma') = [(\gamma')^2 - (\hat{\gamma}'_-)^2]/a_w a_s \ ,$$

which follows from Eq. (13) for $(k_p')^2(z_T')^2/4 \ll 1$. Therefore, making use of Eqs. (19) and (21), the trapped-electron susceptibility can be expressed as

$$\chi_0^T(k',\omega') = \tfrac{1}{2} a_w^2 \hat{\omega}_{pT}^2 \int_{\hat{\gamma}'_-}^{\hat{\gamma}'_+} \frac{d\gamma'}{\gamma'} \frac{\partial \hat{G}_s^T}{\partial \gamma'} \times \sum_{n=-\infty}^{\infty} \frac{(\omega')^2 J_n^2[k' z_T'(\gamma')]}{(\omega')^2 - n^2 \hat{\omega}_B^2(\gamma')} \tag{22}$$

for electrons trapped near the bottom of the ponderomotive potential. In obtaining Eq. (22), we have introduced the renormalized trapped-electron distribution function $\hat{G}_s^T(\gamma')$ defined by[32]

$$G_s^T(\gamma') = \frac{2(a_w a_s)^{1/2}}{mc} \frac{\hat{n}_T}{\hat{n}_b} \hat{G}_s^T(\gamma') \ ,$$
$$\int_{\hat{\gamma}'_-}^{\hat{\gamma}'_+} d\gamma' \gamma' \hat{G}_s^T(\gamma') = 1 \ , \tag{23}$$

where $\hat{\omega}_{pT}^2 = 4\pi \hat{n}_T e^2/m$, and $\hat{n}_T$ is the (spatially averaged) density of trapped electrons. Making use of $\sum_{n=-\infty}^{\infty} J_n^2(x) = 1$, we express the summation in Eq. (22) as

$$\sum_{n=-\infty}^{\infty} \frac{(\omega')^2 J_n^2[k' z_T'(\gamma')]}{(\omega')^2 - n^2 \hat{\omega}_B^2(\gamma')} = 1 + 2 \sum_{n=1}^{\infty} \frac{n^2 \hat{\omega}_B^2(\gamma') J_n^2[k' z_T'(\gamma')]}{(\omega')^2 - n^2 \hat{\omega}_B^2(\gamma')} \ . \tag{24}$$

Making use of Eqs. (9), (22), and (24), and transforming $(\omega',k')$ in the ponderomotive frame to $(\omega,k)$ in the laboratory frame according to Eq. (17), the dispersion relation (19) can be expressed in the compact form

$$\omega^2 - c^2 k^2 - \hat{\alpha}_0 \hat{\omega}_{pb}^2 = -a_w^2 \hat{\omega}_{pT}^2 \sum_{n=1}^{\infty} \int_{\hat{\gamma}'_-}^{\hat{\gamma}'_+} \frac{d\gamma'}{\gamma'} \frac{\partial \hat{G}_s^T}{\partial \gamma'} \frac{n^2 \hat{\omega}_B^2(\gamma') J_n^2[k_L' z_T'(\gamma')]}{\gamma_p^2[\omega - (k+k_0)v_p]^2 - n^2 \hat{\omega}_B^2(\gamma')} \ . \tag{25}$$

In Eq. (25), we have absorbed the dc contribution to $\chi_0^T(k',\omega')$ [i.e., the "1" term in Eq. (24)] into the definition of $\hat{\alpha}_0$. To summarize the pertinent definitions in Eq. (25), we note that

$$a_w = e\hat{B}_w/mc^2 k_0, \quad \hat{\omega}_{pT}^2 = 4\pi \hat{n}_T e^2/m \ ,$$
$$\hat{\omega}_B(\gamma') = [a_w a_s c^2 (k_p')^2/(\gamma')^2]^{1/2}, \quad a_s = e\hat{B}_s/mc^2 k_s \ ,$$
$$k_p' = (k_s + k_0)/\gamma_p, \quad \gamma_p = (1 - v_p^2/c^2)^{-1/2} \ ,$$
$$v_p = \omega_s/(k_s + k_0) \ ,$$
$$(k_p')^2 z_T'^2(\gamma') = [(\gamma')^2 - (\hat{\gamma}'_-)^2]/a_w a_s \ ,$$

and

$$\hat{\gamma}'_\pm = [1 + (a_w \pm a_s)^2]^{1/2} \ .$$

Moreover, the quantity $k_L'(k,\omega)$ occurring in the argument of the Bessel function in Eq. (25) is defined by [see Eq. (17)]

$$k_L' = \gamma_p(k + k_0 - v_p\omega/c^2) \ . \tag{26}$$

In circumstances where the trapped electrons are localized near the bottom of the ponderomotive potential, the stability properties predicted by Eq. (25) are relatively insensitive to the detailed form of $\hat{G}_s^T(\gamma')$.[32] Therefore, for present purposes, we consider the case where the trapped electrons are uniformly distributed in $\gamma'$ from $\gamma' = \hat{\gamma}'_-$ to $\gamma' = \hat{\gamma}'_M$ (Fig. 2), i.e.,

$$\hat{G}_s^T(\gamma') = \begin{cases} \dfrac{2}{(\hat{\gamma}'_M)^2 - (\hat{\gamma}'_-)^2} = \text{const}, & \hat{\gamma}'_- < \gamma' < \hat{\gamma}'_M \\ 0, & \gamma' > \hat{\gamma}'_M \ . \end{cases} \tag{27}$$

Here, the normalization constant is chosen to be consistent with Eq. (23). Moreover, $\hat{\gamma}'_M$ exceeds $\hat{\gamma}'_-$ by only

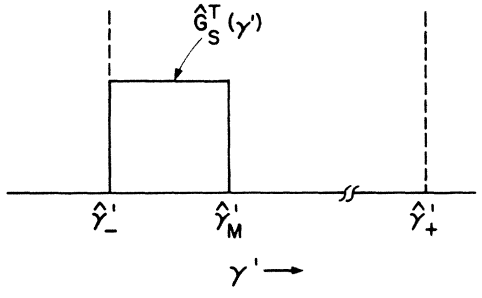


FIG. 2. Plot of trapped-electron distribution function $\hat{G}_S^T(\gamma')$ in Eq. (27) vs $\gamma'$ for electrons trapped near the bottom of the ponderomotive potential.

a small amount so that the trapped-electron distribution is localized near the bottom of the ponderomotive potential with

$$\hat{\gamma}'^2_M - \hat{\gamma}'^2_- \ll \hat{\gamma}'^2_+ - \hat{\gamma}'^2_- = 4a_w a_s \ .$$

Making use of

$$\partial \hat{G}_s^T/\partial\gamma' = \{2/[(\hat{\gamma}'_M)^2-(\hat{\gamma}'_-)^2]\}[\delta(\gamma'-\hat{\gamma}'_-) - \delta(\gamma'-\hat{\gamma}'_M)] \ ,$$

and the fact that $z_T'(\gamma'=\hat{\gamma}'_-)=0$ at the bottom of the well, Eq. (25) becomes

$$\omega^2 - c^2k^2 - \hat{\alpha}_0\hat{\omega}_{pb}^2 = a_w^2\hat{\omega}_{pT}^2 \sum_{n=1}^{\infty} \frac{n^2\Omega_B^2 C_n(k,\omega)}{[\omega-(k+k_0)v_p]^2 - n^2\Omega_B^2} \ , \tag{28}$$

where the effective bounce frequency $\Omega_B$ and the $n$th harmonic coupling coefficient $C_n(k,\omega)$ are defined by

$$\Omega_B^2 = \hat{\omega}_B^2(\gamma'=\hat{\gamma}'_M)/\gamma_p^2 \ , \tag{29}$$

$$C_n(k,\omega) = \left[\frac{2J_n^2[k_L' z_T'(\gamma')]}{\gamma'(\gamma'^2-\hat{\gamma}'^2_-)}\right]_{\gamma'=\hat{\gamma}'_M} \ .$$

The dispersion relation (28) is rich in harmonic content, with resonant behavior occurring on the right-hand side for $\omega-(k+k_0)v_p = \pm n\Omega_B$. Introducing the Doppler-shifted frequency $\Omega$ defined by $\Omega=\omega-(k+k_0)v_p$, Eq. (28) can be expressed in the equivalent form

$$L(\Omega)=R(\Omega) \ , \tag{30}$$

where

$$L(\Omega) = [\Omega+(k+k_0)v_p]^2 - c^2k^2 - \hat{\alpha}_0\hat{\omega}_{pb}^2 \ , \tag{31}$$

$$R(\Omega) = a_w^2\hat{\omega}_{pT}^2 \sum_{n=1}^{\infty} \frac{n^2\Omega_B^2 C_n(k,\omega)}{\Omega^2 - n^2\Omega_B^2} \ .$$

Plots of $L(\Omega)$ and $R(\Omega)$ versus real $\Omega$ are illustrated schematically in Fig. 3 for the case where $L(\Omega)$ is approximated by

$$L(\Omega) = 2(c^2k^2+\hat{\alpha}_0\hat{\omega}_{pb}^2)^{1/2}[\Omega+(k+k_0)v_p - (c^2k^2+\hat{\alpha}_0\hat{\omega}_{pb}^2)^{1/2}] \ ,$$

which corresponds to a forward-propagating electromagnetic wave with

$$\omega \simeq +(c^2k^2+\hat{\alpha}_0\hat{\omega}_{pb}^2)^{1/2} \ .$$

For harmonic numbers $n \geq 2$, note that the $L(\Omega)$ and $R(\Omega)$ curves always intersect, corresponding to stable oscillations with $\mathrm{Im}\Omega=0$. On the other hand, the fundamental ($n=1$) mode may exhibit instability [Fig. 3(a)] or stability [Fig. 3(b)] depending on whether or not the $L(\Omega)$ and $R(\Omega)$ curves intersect in the region $-\Omega_B < \mathrm{Re}\Omega < \Omega_B$ in Fig. 3. The detailed intersection properties in this region are determined by the range of wave number $k$ under consideration.

In the regime of interest for practical applications, $v_p=\omega_s/(k_s+k_0)\approx c$, and the beam density ($\hat{n}_b$) and electromagnetic pump strength ($a_s$) are sufficiently small that the inequalities

$$\frac{\hat{\alpha}_0\hat{\omega}_{pb}^2}{ck}, \ \Omega_B \ll k_0 v_p \tag{32}$$

are satisfied. For example,

$$\Omega_B/ck_0 = [(a_w a_s)^{1/2}/\gamma_p\hat{\gamma}'_M]k_p'/k_0$$

can be approximated by

$$\frac{\Omega_B}{ck_0} = \frac{(a_w a_s)^{1/2}}{\hat{\gamma}'_M}\left[1+\frac{v_p}{c}\right] \ll 1 \tag{33}$$

for $\omega_s \simeq ck_s$ and $a_s \ll 1$. For small $\hat{\omega}_{pT}^2$, and $a_w$ of order unity, the values of $\omega$ and $k$ that solve the dispersion rela-

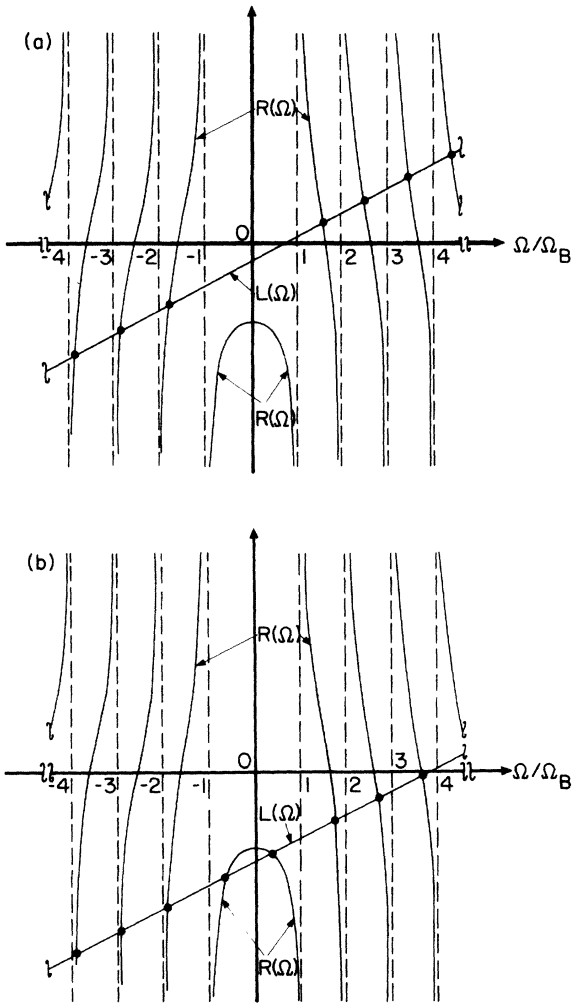


FIG. 3. Plots of $L(\Omega)$ and $R(\Omega)$ vs real $\Omega=\omega-(k+k_0)v_p$ [Eq. (31)]. Points of intersection determine the solutions to $L(\Omega)=R(\Omega)$ [Eq. (30)] corresponding to stable oscillations with $\mathrm{Im}\Omega=0$. In (a), $L(\Omega)$ and $R(\Omega)$ do not intersect in the interval $-\Omega_B<\Omega<\Omega_B$, indicating the existence of instability ($\mathrm{Im}\Omega>0$) in this region. (b) corresponds to stable oscillations ($\mathrm{Im}\Omega=0$) over the entire range of $\Omega$.

tion (28) are closely tuned to the simultaneous resonance conditions

$$\omega = +ck\left[1+\frac{\hat{\alpha}_0\hat{\omega}_{pb}^2}{c^2k^2}\right]^{1/2}, \qquad \omega-(k+k_0)v_p=\pm n\Omega_B\ , \tag{34}$$

where $\hat{\alpha}_0\hat{\omega}_{pb}^2/c^2k^2 \ll 1$ is assumed. We denote the simultaneous solutions to Eq. (34) for $(\omega,k)$ by $(\hat{\omega},\hat{k})$. Making use of $\hat{\alpha}_0\hat{\omega}_{pb}^2/ck \ll k_0v_p$ [Eq. (32)] to solve Eq. (34) iteratively for $(\hat{\omega},\hat{k})$ gives

$$\hat{k}=\gamma_p^2\left[1+\frac{v_p}{c}\right]\frac{v_p}{c}k_0\left[1-\epsilon_b\pm\frac{n\Omega_B}{k_0v_p}\right], \qquad \hat{\omega}=\gamma_p^2\left[1+\frac{v_p}{c}\right]k_0v_p\left[1-\epsilon_b\frac{v_p}{c}\pm\frac{n\Omega_B}{k_0v_p}\right], \tag{35}$$

where $\epsilon_b$ is defined by

$$\epsilon_b=\frac{1}{2}\frac{\hat{\alpha}_0\hat{\omega}_{pb}^2}{k_0^2v_p^2}\frac{1}{\gamma_p^2(1+v_p/c)}\ . \tag{36}$$

Here, the dimensionless parameter $\epsilon_b \ll 1$ describes the shift in wave number and frequency produced by beam dielectric effects. Because $\epsilon_b \ll 1$ and $\Omega_B/k_0c \ll 1$ are assumed [Eq. (32)], we note from Eq. (35) that beam dielectric effects ($\epsilon_b$) and the bounce motion of the trapped electrons ($\pm n\Omega_B/k_0v_p$) produce very small shifts in wave number and frequency relative to the central values $(\hat{\omega}_c,\hat{k}_c)$ defined by

$$\hat{k}_c=\gamma_p^2\left[1+\frac{v_p}{c}\right]\frac{v_p}{c}k_0\ , \qquad \hat{\omega}_c=\gamma_p^2\left[1+\frac{v_p}{c}\right]k_0v_p\ . \tag{37}$$

Moreover, adjacent sideband modes in Eq. (35) are separated in frequency by an amount equal to $\gamma_b^2(1+v_p/c)\Omega_B$.

Finally, for the case where the trapped electrons are localized near the bottom of the ponderomotive potential, it is readily shown that

$$(k_L')^2z_T'^2(\gamma'=\hat{\gamma}'_M) =[(k_L')^2/(k_p')^2]\{[(\hat{\gamma}'_M)^2-(\hat{\gamma}'_-)^2]/a_wa_s\} \ll 1$$

in Eq. (28). Therefore, using the small-argument expansion $J_n(x)\simeq(n!)^{-1}(x/2)^n$, it follows from Eq. (29) that the factor $n^2\Omega_B^2C_n(k,\omega)$ occurring in the dispersion relation (28) can be approximated by

$$n^2\Omega_B^2C_n(k,\omega)=\frac{c^2(k_L')^2}{2(\hat{\gamma}'_M)^3\gamma_p^2}\frac{n^2}{(n!)^2}\times\left[\frac{(k_L')^2z_T'^2(\gamma'=\hat{\gamma}'_M)}{4}\right]^{n-1}, \tag{38}$$

where $k_L'(k,\omega)$ is defined in Eq. (26). Evidently, because

$$(k_L')^2z_T'^2(\gamma'=\hat{\gamma}'_M)/4 \ll 1\ ,$$

it follows from Eq. (38) that $n^2\Omega_B^2C_n(k,\omega)$ decreases rapidly with increasing $n$ for harmonic numbers $n \geq 2$. This property, peculiar to the case where the trapped electrons are localized near the bottom of the ponderomotive potential, allows us to neglect all $n \geq 2$ harmonic contributions in Eq. (28) when calculating the stability behavior associated with the fundamental ($n=1$) mode. Furthermore, for the (stable) oscillations at the higher harmonic numbers $n \geq 2$, the simultaneous resonance conditions in Eq. (34) provide an excellent estimate of the oscillation frequency and wave number when $(k_L')^2z_T'^2(\gamma'=\hat{\gamma}'_M)/4 \ll 1$.

### B. Sideband instability for the fundamental ($n=1$) mode

Based on the discussion at the end of Sec. III A, we now consider the fundamental ($n=1$) mode and neglect all harmonic contributions in Eq. (28) for $n \geq 2$. Therefore, making use of Eq. (38), the dispersion relation (28) is approximated by

$$\{[\omega-(k+k_0)v_p]^2-\Omega_B^2\}(\omega^2-c^2k^2-\hat{\alpha}_0\hat{\omega}_{pb}^2) =a_w^2\hat{\omega}_{pT}^2\Omega_B^2C_1(k,\omega)=\frac{a_w^2\hat{\omega}_{pT}^2c^2(k_L')^2}{2(\hat{\gamma}'_M)^3\gamma_p^2}\ , \tag{39}$$

where $k_L'=\gamma_p(k+k_0-v_p\omega/c^2)$. We introduce the dimensionless parameter $\Gamma_0 \ll 1$ defined by

$$\Gamma_0^3\equiv\frac{a_w^2\hat{\omega}_{pT}^2c^2(\hat{k}'_L)^2}{4\hat{\omega}_cc^3k_0^3(\hat{\gamma}'_M)^3\gamma_p^2}\ , \tag{40}$$

where $\hat{k}'_L$ is defined by

$$\hat{k}'_L\equiv(\hat{k}_c+k_0)/\gamma_p=\gamma_p(1+v_p/c)k_0\ .$$

Here, without loss of generality, $\hat{\omega}_c$ and $\hat{k}_c$ exactly solve the simultaneous resonance conditions, $\hat{\omega}_c-(\hat{k}_c+k_0)v_p=0$ and $\hat{\omega}_c=c\hat{k}_c$, which give the expressions in Eq. (37). Expressing $\omega=\hat{\omega}_c+\delta\omega$ and $k=\hat{k}_c+\delta k$, and making use of $k_L'=\gamma_p(k+k_0-v_p\omega/c^2)$, it is straightforward to show that the dispersion relation (39) can be expressed (exactly) as

$$[(\delta\omega-v_p\delta k)^2-\Omega_B^2]\left[(\delta\omega-v_p\delta k)-ck_0\frac{v_p}{c}\left[\frac{\delta k}{\hat{k}_c}+\frac{\hat{\alpha}_0\hat{\omega}_{pb}^2}{2k_0\hat{k}_cv_pc}\right]+\frac{(\delta\omega-v_p\delta k)^2}{2c\hat{k}_c}+\frac{v_p}{c}(\delta\omega-v_p\delta k)\frac{\delta k}{\hat{k}_c}-\frac{c(\delta k)^2}{2\gamma_p^2\hat{k}_c}\right] =\Gamma_0^3c^3k_0^3\left[1+\frac{v_p}{c}\frac{\delta k}{\hat{k}_c}-\frac{v_p/c}{1+v_p/c}\frac{(\delta\omega-v_p\delta k)}{ck_0}\right]^2, \tag{41}$$

where use has been made of the definitions of $\hat{k}_c$ and $\hat{\omega}_c$ in Eq. (37).

For $\Gamma_0 \ll 1$ and $\Omega_B/ck_0 \ll 1$, the solutions to Eq. (41) satisfy $|\delta\omega - v_p\delta k| \ll k_0 c \ll \hat{k}_c c$ and $|\delta k| \ll \hat{k}_c$. Therefore, an excellent approximation to Eq. (41) is given by

$$[(\delta\omega - v_p\delta k)^2 - \Omega_B^2]\left[(\delta\omega - v_p\delta k) - ck_0\frac{v_p}{c}\left[\frac{\delta k}{\hat{k}_c} + \epsilon_b\right]\right] = \Gamma_0^3 c^3 k_0^3 , \tag{42}$$

where

$$\epsilon_b = \hat{\alpha}_0\hat{\omega}_{pb}^2/2k_0\hat{k}_c v_p c$$
$$= (\hat{\alpha}_0\hat{\omega}_{pb}^2/2\gamma_p^2 k_0^2 v_p^2)(1+v_p/c)^{-1}$$

is the small parameter ($\epsilon_b \ll 1$) defined in Eq. (36). Here, $\Gamma_0$ is defined in Eq. (40), and $\hat{k}_c$ is defined by

$$\hat{k}_c = \gamma_p^2(1+v_p/c)(v_p/c)k_0 .$$

It is convenient to introduce the dimensionless frequency shift $\delta\tilde{\Omega}$, bounce frequency $\tilde{\Omega}_B$, and wave number shift $\delta\tilde{K}$ defined by

$$\delta\tilde{\Omega} = \frac{(\delta\omega - v_p\delta k)}{\Gamma_0 k_0 c} ,$$
$$\tilde{\Omega}_B = \frac{\Omega_B}{\Gamma_0 k_0 c} , \tag{43}$$
$$\delta\tilde{K} = \frac{v_p}{\Gamma_0 c}\left[\frac{\delta k}{\hat{k}_c} + \epsilon_b\right] .$$

The dispersion relation (42) can then be expressed in the equivalent form

$$[(\delta\tilde{\Omega})^2 - \tilde{\Omega}_B^2](\delta\tilde{\Omega} - \delta\tilde{K}) = 1 . \tag{44}$$

Equation (44) is the final form of the approximate dispersion relation describing the sideband instability for the fundamental ($n=1$) mode. To summarize briefly, in deriving Eq. (44) it has been assumed that

$$\Omega_B/ck_0 = [a_W a_s/(\hat{\gamma}'_M)^2]^{1/2}(1+v_p/c) \ll 1$$

[Eq. (33)] and that $\Gamma_0 \ll 1$ [Eq. (40)]. Making use of

$$\hat{k}_c = \gamma_p^2(1+v_p/c)(v_p/c)k_0, \quad \hat{\omega}_c = c\hat{k}_c ,$$
$$\hat{k}'_L = (\hat{k}_c + k_0)/\gamma_p = \gamma_p(1+v_p/c)k_0 ,$$

and $\hat{\gamma}'_M \simeq (1+a_w^2)^{1/2}$, it is readily shown that $\Gamma_0^3$ can be expressed as

$$\Gamma_0^3 = \frac{1}{4}\frac{a_w^2}{(1+a_w^2)^{3/2}}\frac{\hat{\omega}_{pT}^2}{\gamma_p^2 c^2 k_0^2}\frac{(1+v_p/c)}{v_p/c} \ll 1 . \tag{45}$$

The inequality in Eq. (45) is easily satisfied for the practical case of a tenuous electron beam with $\hat{\omega}_{pT}^2/\gamma_p^2 c^2 k_0^2 \ll 1$.

As an important notational point, we note that the trapped electron density in the pondermotive frame ($\hat{n}_T$) is related to the trapped electron density in the laboratory frame ($n_T$) by $\hat{n}_T = n_T/\gamma_p$. [Similarly, $\hat{n}_b = n_b/\gamma_p$ for the total beam density.] Therefore, factors such as $\hat{\omega}_{pT}^2/\gamma_p^2 c^2 k_0^2 = 4\pi\hat{n}_T e^2/\gamma_p^2 mc^2 k_0^2$ occurring in Eq. (45) can be expressed in the more familiar form

$$\frac{\hat{\omega}_{pT}^2}{\gamma_p^2 c^2 k_0^2} = \frac{(4\pi n_T e^2/m)}{\gamma_p^3 c^2 k_0^2} ,$$

where $n_T$ is the average trapped electron density in the laboratory frame.

In dimensionless variables, Eq. (44) is a cubic equation which determines the complex oscillation frequency $\delta\tilde{\Omega}$ in terms of the wave number $\delta\tilde{K}$. Note that the dimensionless parameter $\tilde{\Omega}_B = (\Omega_B/ck_0)/\Gamma_0$ is the ratio of two small parameters, $\Omega_B/ck_0$ and $\Gamma_0$. Therefore, $\tilde{\Omega}_B$ can cover the range from $\tilde{\Omega}_B \ll 1$ (weak-pump regime) to $\tilde{\Omega}_B \gg 1$ (strong-pump regime).

### C. Analysis of dispersion relation

A detailed investigation of the dispersion relation (44) over a wide range of $\tilde{\Omega}_B$ shows that the maximum growth rate occurs for frequency and wave number in the vicinity of

$$\delta\tilde{\Omega} \approx -\tilde{\Omega}_B ,$$
$$\delta\tilde{K} \approx -\tilde{\Omega}_B . \tag{46}$$

Note that Eq. (46) corresponds to the resonant frequency and wave number $(\hat{\omega},\hat{k})$ defined in Eq. (35) for the *lower* sideband (minus sign) of the fundamental ($n=1$) mode. We therefore introduce the shifted dimensionless frequency and wave number $\delta\tilde{\Omega}'$ and $\delta\tilde{K}'$ defined by

$$\delta\tilde{\Omega} = -\tilde{\Omega}_B + \delta\tilde{\Omega}' ,$$
$$\delta\tilde{K} = -\tilde{\Omega}_B + \delta\tilde{K}' . \tag{47}$$

Making use of Eq. (47), the dispersion relation (44) can be expressed in the equivalent form

$$(\delta\tilde{\Omega}')(\delta\tilde{\Omega}' - 2\tilde{\Omega}_B)(\delta\tilde{\Omega}' - \delta\tilde{K}') = 1 . \tag{48}$$

Because maximum growth occurs for $\delta\tilde{K}' \approx 0$, we solve Eq. (48) for the case $\delta\tilde{K}' = 0$ exactly. The solution to $(\delta\tilde{\Omega}')^3 - 2\tilde{\Omega}_B(\delta\tilde{\Omega}')^2 - 1 = 0$ then determines the characteristic maximum growth rate $\mathrm{Im}(\delta\tilde{\Omega}') = \mathrm{Im}(\delta\tilde{\Omega}) = \mathrm{Im}(\delta\omega)/\Gamma_0 k_0 c$. Some straightforward algebra gives

$$\mathrm{Im}(\delta\omega) = \Gamma_0 k_0 c\frac{(3)^{1/2}}{(2)^{5/3}}\left[1+\frac{32}{27}\frac{\Omega_B^3}{\Gamma_0^3 k_0^3 c^3}\right]^{1/3}\left\{\left[1+\left[1+\frac{32}{27}\frac{\Omega_B^3}{\Gamma_0^3 k_0^3 c^3}\right]^{-1/2}\right]^{2/3} - \left[1-\left[1+\frac{32}{27}\frac{\Omega_B^3}{\Gamma_0^3 k_0^3 c^3}\right]^{-1/2}\right]^{2/3}\right\} \tag{49}$$

for $\delta\tilde{K}'=0$, which corresponds to

$$k=\hat{k}=\gamma_p^2(1+v_p/c)(v_p/c)k_0[1-\epsilon_b-\Omega_B/k_0v_p] .$$

[See Eqs. (35), (43), and (47).] In the weak-pump regime ($\tilde{\Omega}_B \ll 1$), Eq. (49) reduces to

$$\mathrm{Im}(\delta\omega)=\frac{(3)^{1/2}}{2}\Gamma_0 k_0 c, \quad \text{for } \Omega_B \ll \Gamma_0 k_0 c . \tag{50}$$

On the other hand, in the strong-pump regime ($\tilde{\Omega}_B \gg 1$), Eq. (49) gives

$$\mathrm{Im}(\delta\omega)=\frac{\Gamma_0 k_0 c}{(2)^{1/2}}\left[\frac{\Gamma_0 k_0 c}{\Omega_B}\right]^{1/2}, \quad \text{for } \Omega_B \gg \Gamma_0 k_0 c . \tag{51}$$

Figure 4 shows a plot of $\mathrm{Im}(\delta\omega)/[(3)^{1/2}\Gamma_0 k_0 c/2]$ versus the normalized pump strength $\tilde{\Omega}_B=\Omega_B/\Gamma_0 k_0 c$ calculated from Eq. (49). It is evident from Fig. 4 that $\mathrm{Im}(\delta\omega)$ exhibits a simple scaling with $\Omega_B/\Gamma_0 k_0 c$ only in the asymptotic limits in Eqs. (50) and (51).

The dispersion relation (48) assumes a particularly simple form in the strong-pump limit ($\tilde{\Omega}_B \gg 1$). Assuming $|\delta\tilde{\Omega}'| \ll 2\tilde{\Omega}_B$, Eq. (48) can be approximated by the quadratic equation

$$(\delta\tilde{\Omega}')^2-(\delta\tilde{K}')(\delta\tilde{\Omega}')+\frac{1}{2\tilde{\Omega}_B}=0 . \tag{52}$$

The solution to Eq. (52) is given by

$$\delta\tilde{\Omega}'=\frac{1}{2}\left[(\delta\tilde{K}')\pm\left[(\delta\tilde{K}')^2-\frac{2}{\tilde{\Omega}_B}\right]^{1/2}\right] . \tag{53}$$

The unstable branch in Eq. (53) exhibits instability ($\mathrm{Im}\delta\tilde{\Omega}'>0$) for $\delta\tilde{K}'$ satisfying

$$|\delta\tilde{K}'|<\delta\tilde{K}'_M\equiv\frac{(2)^{1/2}}{\tilde{\Omega}_B^{1/2}}=\left[\frac{2\Gamma_0 k_0 c}{\Omega_B}\right]^{1/2} . \tag{54}$$

The corresponding growth rate obtained from Eq. (53) is

$$\mathrm{Im}(\delta\omega)=\frac{\Gamma_0 k_0 c}{(2)^{1/2}}\left[\frac{\Gamma_0 k_0 c}{\Omega_B}\right]^{1/2}\left[1-\frac{(\delta\tilde{K}')^2}{(\delta\tilde{K}'_M)^2}\right]^{1/2} , \tag{55}$$

with maximum growth [Eq. (51)] occurring for $\delta\tilde{K}'=0$. We note from Eq. (55) that the full bandwidth of the instability is $2(\delta\tilde{K}'_M)$. From Eqs. (43), (47), and (54), the corresponding bandwidth in $k$ space ($\Delta k$) is given by

$$\frac{\Delta k}{\hat{k}_c}=2\Gamma_0\frac{c}{v_p}\left[\frac{2\Gamma_0 k_0 c}{\Omega_B}\right]^{1/2} , \tag{56}$$

where $\hat{k}_c=\gamma_p^2(1+v_p/c)(v_0/c)k_0$ is defined in Eq. (37).

Of course the complex oscillation frequency

$$\delta\tilde{\Omega}=(\delta\omega-v_p\delta k)/\Gamma_0 k_0 c$$

can be determined exactly from the cubic dispersion relation (44) [or equivalently, Eq. (48)] for general values of the dimensionless pump parameter $\tilde{\Omega}_B=\Omega_B/\Gamma_0 k_0 c$ and wave number

$$\delta\tilde{K}=(v_p/\Gamma_0 c)(\delta k/\hat{k}_c+\epsilon_b) .$$

Typical numerical results are illustrated in Figs. 5 and 6. Shown in Fig. 5 are plots of $\mathrm{Im}(\delta\tilde{\Omega})$ [Fig. 5(a)] and $\mathrm{Re}(\delta\tilde{\Omega})$ [Fig. 5(b)] versus $\delta\tilde{K}$ calculated from Eq. (44) for $\tilde{\Omega}_B=1$. Note from Fig. 5(a) that the growth rate $\mathrm{Im}(\delta\omega)$ assumes the maximum value $\mathrm{Im}(\delta\omega)\simeq 0.67\Gamma_0 k_0 c$ for $\delta\tilde{K}\simeq -0.8\tilde{\Omega}_B$. Moreover, $\mathrm{Re}(\delta\tilde{\Omega})$ varies approximately linearly with $\delta\tilde{K}$ over the unstable range $-2.3<\delta\tilde{K}<0.8$.

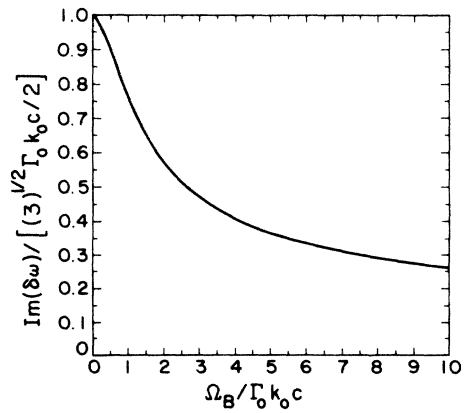


FIG. 4. Plots of normalized growth rate $\mathrm{Im}(\delta\omega)/[(3)^{1/2}\Gamma_0 k_0 c/2]$ vs dimensionless pump strength $\Omega_B/\Gamma_0 k_0 c$ for $\delta\tilde{K}'=0$ [Eq. (49)].

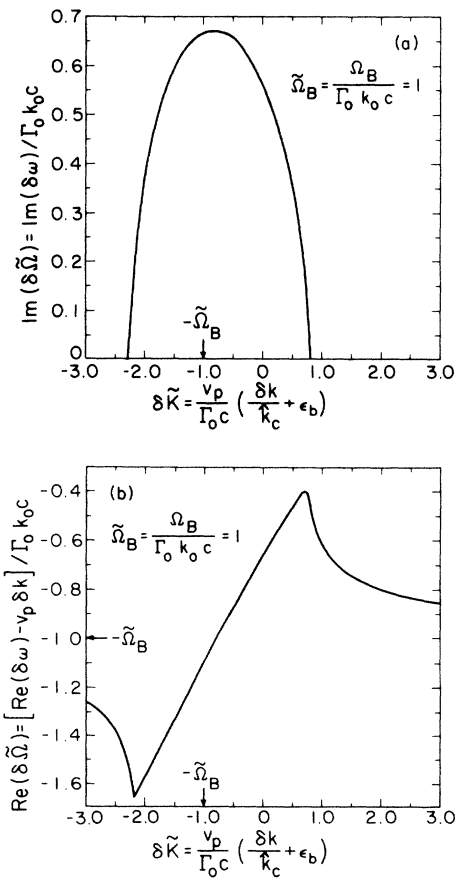


FIG. 5. Plots of (a) $\mathrm{Im}(\delta\omega)/\Gamma_0 k_0 c$ and (b) $[\mathrm{Re}(\delta\omega)-v_p\delta k]/\Gamma_0 k_0 c$ vs $\delta\tilde{K}=(v_p/\Gamma_0 c)(\delta k/\hat{k}_c+\epsilon_b)$ calculated from Eq. (44) for dimensionless pump strength $\Omega_B/\Gamma_0 k_0 c=1$.

To illustrate the dependence of the instability growth rate and bandwidth on $\tilde{\Omega}_B$, shown in Fig. 6 are plots of $\mathrm{Im}(\delta\tilde{\Omega})$ versus $\delta\tilde{K}$ calculated from Eq. (44) for $\tilde{\Omega}_B=0.2$, 2, 5, 7, and 10. For a weak pump with $\tilde{\Omega}_B=0.2$, we note from Fig. 6 that the maximum growth rate is $\mathrm{Im}(\delta\omega)=0.86\Gamma_0 k_0 c$ for $\delta\tilde{K}\simeq 0$, and that the instability bandwidth in $\delta\tilde{K}$ space is quite broad. On the other hand, as $\tilde{\Omega}_B$ is increased to values exceeding unity, the maximum growth rate in Fig. 6 decreases [see Fig. 4 and Eq. (49)]; the bandwidth in $\delta\tilde{K}$ space decreases [see Eq. (54)]; and the value of $\delta\tilde{K}$ at maximum growth corresponds to $\delta\tilde{K}\simeq-\tilde{\Omega}_B$ [see Eq. (46)]. Indeed, for $\tilde{\Omega}_B\gg 1$, the approximate dispersion relation (53) provides an excellent description of stability properties. For example, for $\tilde{\Omega}_B=10$ in Fig. 6, the maximum growth rate $\mathrm{Im}(\delta\omega)\simeq 0.22\Gamma_0 k_0 c$ and bandwidth $2(\delta\tilde{K})_M=0.95$ calculated numerically from the cubic dispersion relation (44) are in excellent agreement with the estimates in Eqs. (54) and (55).

To summarize the key results in the strong-pump ($\Omega_B\gg\Gamma_0 k_0 c$) and weak-pump ($\Omega_B\ll\Gamma_0 k_0 c$) regimes, the following points are noteworthy. First, the characteristic growth rate in the weak-pump regime [Eq. (50)] is independent of pump strength (as measured by $\Omega_B$), whereas the growth rate in the strong-pump regime [Eq. (51)] scales as $\mathrm{Im}(\delta\omega)\propto\Omega_B^{-1/2}\propto a_s^{-1/4}$. Moreover, for specified $\Gamma_0 k_0 c$, the characteristic growth rate in the strong-pump regime [Eq. (51)] is smaller by a factor $(2\Gamma_0 c k_0/3\Omega_B)^{1/2}$ than the growth rate in the weak-pump regime [Eq. (50)]. It is also evident from Eq. (54) and Fig. 6 that the bandwidth of the sideband instability in $\delta K$ space is greatly reduced in the strong-pump regime where $\Omega_B/\Gamma_0 k_0 c\gg 1$.

Finally, as an illustrative set of system parameters, we consider the case where

$$\begin{aligned}&\lambda_0=6.28\ \mathrm{cm},\quad k_0=1\ \mathrm{cm}^{-1},\\ &\hat{B}_w=1.70\ \mathrm{kG},\quad a_w=1,\\ &\hat{n}_T=3.14\times10^8\ \mathrm{cm}^{-3},\quad \hat{\omega}_{pT}=10^9\ \mathrm{s}^{-1},\\ &\gamma_p=40,\quad \hat{\gamma}'_M\simeq(1+a_w^2)^{1/2}=1.414.\end{aligned}\tag{57}$$

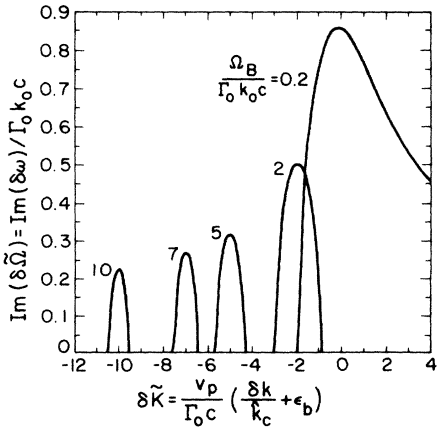


FIG. 6. Plots of $\mathrm{Im}(\delta\omega)/\Gamma_0 k_0 c$ vs $\delta\tilde{K}=(v_p/\Gamma_0 c)(\delta k/\hat{k}_c+\epsilon_b)$ calculated from Eq. (44) for $\Omega_B/\Gamma_0 k_0 c=0.2$, 2, 5, 7, and 10. Maximum growth rate occurs for $\delta\tilde{K}\approx-\Omega_B/\Gamma_0 k_0 c$ [Eq. (46)].

Some straightforward algebra that makes use of Eqs. (33), (45), and (57) gives $\Gamma_0^3=12.3\times10^{-8}$ and $\Omega_B/ck_0=(2a_s)^{1/2}$, which reduce to

$$\begin{aligned}&\Gamma_0=4.97\times10^{-3},\\ &\frac{\Omega_B}{ck_0}=1.414(a_s)^{1/2}.\end{aligned}\tag{58}$$

Therefore, for the choice of parameters in Eq. (57), it follows from Eq. (58) that

$$\frac{\Omega_B}{\Gamma_0 c k_0}\gtrless 1\tag{59}$$

accordingly as

$$a_s\gtrless 1.24\times10^{-5}.\tag{60}$$

That is, for primary electromagnetic wave amplitude sufficiently large that $a_s>1.24\times10^{-5}$, the sideband instability operates in the strong-pump regime with $\Omega_B/\Gamma_0 c k_0>1$.

From Eqs. (2) and (3), it follows that the radiation power flow per unit area associated with the primary electromagnetic wave $(\omega_s,k_s)$ is given by

$$P_s/A_s=c(\omega_s/ck_s)\hat{B}_s^2/4\pi.$$

For $\omega_s\simeq ck_s$, the quantity $P_s/A_s$ can also be expressed as

$$\frac{P_s}{A_s}=7.7\times10^{-11}\omega_s^2 a_s^2\ \frac{\mathrm{W}}{\mathrm{cm}^2},\tag{61}$$

where $a_s=e\hat{B}_s/mc^2k_s$. For the parameters in Eq. (57), we estimate

$$\omega_s\simeq 2\gamma_p^2 ck_0=9.6\times10^{13}\ \mathrm{s}^{-1},$$

and Eq. (61) becomes

$$\frac{P_s}{A_s}=7.1\times10^{17}a_s^2\ \frac{\mathrm{W}}{\mathrm{cm}^2}.\tag{62}$$

As an example, we take the effective area of the radiation channel to be $A_s=\pi r_s^2=0.0628\ \mathrm{cm}^2$ corresponding to $r_s=1.414$ mm. Then for $a_s=1.24\times10^{-5}$ [Eq. (60)], Eq. (62) gives $P_s=6.9$ MW. That is, for $A_s=0.0628\ \mathrm{cm}^2$ and the choice of parameters in Eq. (57), the strong-pump regime ($\Omega_B/\Gamma_0 c k_0>1$) corresponds to $P_s>6.9$ MW. Moreover, for $ck_s=9.6\times10^{13}\ \mathrm{s}^{-1}$, the condition $a_s>1.24\times10^{-5}$ corresponds to $\hat{B}_s>68$ G. [Compare with the strength of the wiggler field $\hat{B}_w=1.70$ kG in Eq. (57).]

## IV. CONCLUSIONS

Making use of a kinetic formalism[32] based on the Vlasov-Maxwell equations, we have investigated detailed properties of the sideband instability for the case where the trapped electrons are localized near the bottom of the ponderomotive potential. Following a summary of the theoretical model and assumptions (Sec. II), we obtained the dispersion relation (25), which neglects the effects of the untrapped electrons and is valid for general distribution $\hat{G}_s^T(\gamma')$ of trapped electrons localized near the bot-

tom of the ponderomotive potential. For the choice of uniform distribution function $\hat{G}_s^T(\gamma')$ in Eq. (27), the dispersion relation (25) reduced to Eq. (28), which exhibits stable sideband oscillations ($\mathrm{Im}\omega=0$) for all harmonic numbers $n \geq 2$ (Sec. III A). In Secs. III B and III C, neglecting the harmonic contributions for $n \geq 2$, use was made of the dispersion relation (39) to investigate detailed properties of the sideband instability for the fundamental ($n=1$) mode. For $\Omega_B/ck_0 \ll 1$ and $\Gamma_0 \ll 1$ (the regime of practical interest), Eq. (39) was approximated by Eq. (44) [or equivalently, Eq. (48)], which determines the dimensionless frequency shift $\delta\tilde{\Omega}=(\delta\omega-v_p\delta k)/\Gamma_0 k_0 c$ in terms of the normalized pump strength $\tilde{\Omega}_B=\Omega_B/\Gamma_0 k_0 c$ and the dimensionless wave-number shift

$$\delta\tilde{K}=(v_p/\Gamma_0 c)(\delta k/\hat{k}_c+\epsilon_b) .$$

Here, $\delta k=k-\hat{k}_c$ and $\delta\omega=\omega-\hat{\omega}_c$, where

$$\hat{k}_c=\gamma_p^2(1+v_p/c)(v_p/c)k_0$$

and $\hat{\omega}_c=\hat{k}_c c$. As a general remark, it was found that instability exists ($\mathrm{Im}\delta\omega>0$) for $(\omega,k)$ in the vicinity of $(\hat{\omega},\hat{k})$ defined by

$$\hat{k}=\gamma_p^2\left[1+\frac{v_p}{c}\right]\frac{v_p}{c}k_0\left[1-\epsilon_b-\frac{\Omega_B}{k_0 v_p}\right] ,$$

$$\hat{\omega}=\gamma_p^2\left[1+\frac{v_p}{c}\right]k_0 v_p\left[1-\epsilon_b\frac{v_p}{c}-\frac{\Omega_B}{k_0 v_p}\right] ,$$

which corresponds to the *lower* sideband in Eq. (35) for the fundamental ($n=1$) mode. Moreover, it was found that the corresponding growth rate $\mathrm{Im}(\delta\omega)$ and instability bandwidth (in $\delta k$ space) exhibit a sensitive dependence on the normalized pump strength $\Omega_B/\Gamma_0 k_0 c$ [Fig. 6 and Eq. (49)]. For example, in the weak-pump regime ($\Omega_B/\Gamma_0 k_0 c \ll 1$), the instability is relatively broadband, and the characteristic maximum growth rate is [Eq. (50)]

$$\mathrm{Im}(\delta\omega)=\frac{(3)^{1/2}}{2}\Gamma_0 k_0 c .$$

On the other hand, in the strong-pump regime ($\Omega_B/\Gamma_0 k_0 c \gg 1$), the characteristic maximum growth rate is [Eq. (51)]

$$\mathrm{Im}(\delta\omega)=\frac{\Gamma_0 k_0 c}{(2)^{1/2}}\left[\frac{\Gamma_0 k_0 c}{\Omega_B}\right]^{1/2} ,$$

and the corresponding bandwidth is relatively narrow [Eq. (56)]. Note from Eqs. (50) and (51) that the growth rate of the sideband instability is greatly reduced as the dimensionless pump strength is increased to the regime where $\Omega_B/\Gamma_0 k_0 c \gg 1$.

As a final point, the dispersion relation (25) and related analysis in Sec. III are valid for electromagnetic wave perturbations with *right-circular* polarization, in which case it is found that only the *lower* sideband exhibits instability. A completely parallel analysis can be carried out in circumstances where the wave perturbations have *left-circular* polarization.[32] In this case, it is found[32] that the role of the lower and the upper sidebands is reversed, and the *upper* sideband exhibits instability for perturbations with left-circular polarization.

## ACKNOWLEDGMENTS

It is a pleasure to acknowledge the benefit of useful discussions with William M. Sharp. This research was supported by Los Alamos National Laboratory and in part by the Office of Naval Research.

[1]V. P. Sukhatme and P. A. Wolff, J. Appl. Phys. **44**, 2331 (1973).
[2]W. B. Colson, Phys. Lett. **59A**, 187 (1976).
[3]A. Hasegawa, Bell Syst. Tech. J. **57**, 3069 (1978).
[4]N. M. Kroll and W. A. McMullin, Phys. Rev. A **17**, 300 (1978).
[5]L. R. Elias, W. M. Fairbank, J. M. J. Madey, H. A. Schwettman, and T. I. Smith, Phys. Rev. Lett. **36**, 717 (1976).
[6]D. A. G. Deacon, L. R. Elias, J. M. J. Madey, G. J. Ramian, H. A. Schwettman, and T. I. Smith, Phys. Rev. Lett. **38**, 892 (1977).
[7]D. B. McDermott, T. C. Marshall, S. P. Schlesinger, R. K. Parker, and V. L. Granatstein, Phys. Rev. Lett. **41**, 1368 (1978).
[8]A. N. Didenko, A.R. Borisov, G. R. Fomenko, A. V. Kosevnikov, G. V. Melnikov, Yu G. Stein, and A. G. Zerlitsin, IEEE Trans. Nucl. Sci. **NS-28**, 3169 (1981).
[9]S. Benson, D. A. G. Deacon, J. N. Eckstein, J. M. J. Madey, K. Robinson, T. I. Smith, and R. Taber, Phys. Rev. Lett. **48**, 235 (1982).
[10]R. K. Parker, R. H. Jackson, S. H. Gold, H. P. Freund, V. L. Granatstein, P. C. Efthimion, M. Herndon, and A. K. Kinkead, Phys. Rev. Lett. **48**, 238 (1982).
[11]D. Prosnitz and A. M. Sessler, in *Physics of Quantum Electronics* (Addison-Wesley, Reading, Mass., 1982), Vol. 9, p. 651.
[12]A. Grossman, T. C. Marshall, and S. P. Schlesinger, Phys. Fluids **26**, 337 (1983).
[13]C. W. Roberson, J. A. Pasour, F. Mako, R. F. Lucey, Jr., and P. Sprangle, Infrared Millimeter Waves **10**, 361 (1983), and references therein.
[14]G. Bekefi, R. E. Shefer, and W. W. Destler, Appl. Phys. Lett. **44**, 280 (1983).
[15]R. W. Warren, B. E. Newman, J. G. Winston, W.E. Stein, L. M. Young, and C. A. Brau, IEEE J. Quantum Electron. **QE-19**, 391 (1983).
[16]R. W. Warren, B. E. Newnam, and J. C. Goldstein, IEEE J. Quantum Electron. **QE-21**, 882 (1985).
[17]T. J. Orzechowski, B. Anderson, W. M. Fawley, D. Prosnitz, E. T. Scharlemann, S. Yarema, D. B. Hopkins, A. C. Paul, A. M. Sessler, and J. S. Wurtele, Phys. Rev. Lett. **54**, 889 (1985).
[18]T. J. Orzechowski, E. T. Scharlemann, B. Anderson, V. K. Neil, W. M. Fawley, D. Prosnitz, S. M. Yarema, D. B. Hop-

kins, A. C. Paul, A. M. Sessler, and J. S. Wurtele, IEEE J. Quantum Electron. **QE-21**, 831 (1985).
[19]J. Fajans, G. Bekefi, Y. Z. Yin, and B. Lax, Phys. Rev. Lett. **53**, 246 (1984).
[20]F. A. Hopf, P. Meystre, M. O. Scully, and W. H. Louisell, Phys. Rev. Lett. **37**, 1342 (1976).
[21]W. H. Louisell, J. F. Lam, D. A. Copeland, and W. B. Colson, Phys. Rev. A **19**, 288 (1979).
[22]P. Sprangle, C. M. Tang, and W. M. Manheimer, Phys. Rev. A **21**, 302 (1980).
[23]W. B. Colson, IEEE J. Quantum Electron. **QE-17**, 1417 (1981).
[24]N. M. Kroll, P. L. Morton, and M. N. Rosenbluth, IEEE J. Quantum Electron. **QE-17**, 1436 (1981).
[25]T. Taguchi, K. Mima, and T. Mochizuki, Phys. Rev. Lett. **46**, 824 (1981).
[26]J. C. Goldstein and W. B. Colson, *Proceedings of the International Conference on Lasers*, (STS, McLean, VA, 1982), p. 218.
[27]N. S. Ginzburg and M. A. Shapiro, Opt. Commun. **40**, 215 (1982).
[28]R. C. Davidson and W. A. McMullin, Phys. Rev. A **26**, 410 (1982).
[29]B. Lane and R. C. Davidson, Phys. Rev. A **27**, 2008 (1983).
[30]A. M. Dimos and R. C. Davidson, Phys. Fluids **28**, 677 (1985).
[31]R. C. Davidson and Y. Z. Yin, Phys. Fluids **28**, 2524 (1985).
[32]R. C. Davidson, Phys. Fluids **29**, 2689 (1986).
[33]H. S. Uhm and R. C. Davidson, Phys. Fluids **24**, 2348 (1981).
[34]R. C. Davidson and H. S. Uhm, J. Appl. Phys. **53**, 2910 (1982).
[35]H. S. Uhm and R. C. Davidson, Phys. Fluids **26**, 288 (1983).
[36]H. P. Freund and A. K. Ganguly, Phys. Rev. A **28**, 3438 (1983).
[37]G. L. Johnston and R. C. Davidson, J. Appl. Phys. **55**, 1285 (1984).
[38]R. C. Davidson and Y. Z. Yin, Phys. Rev. A **30**, 3078 (1984).
[39]W. A. McMullin and G. Bekefi, Appl. Phys. Lett. **39**, 845 (1981).
[40]R. C. Davidson and W. A. McMullin, Phys. Rev. A **26**, 1997 (1982).
[41]W. A. McMullin and G. Bekefi, Phys. Rev. A **25**, 1826 (1982).
[42]R. C. Davidson and W. A. McMullin, Phys. Fluids **26**, 840 (1983).
[43]R. C. Davidson, W. A. McMullin, and K. Tsang, Phys. Fluids **27**, 233 (1983).
[44]T. Kwan, J. M. Dawson, and A. T. Lin, Phys. Fluids **20**, 581 (1977).
[45]T. Kwan and J. M. Dawson, Phys. Fluids **22**, 1089 (1979).
[46]I. B. Bernstein and J. L. Hirschfield, Physica (Utrecht) **20A**, 1661 (1979).
[47]P. Sprangle and R. A. Smith, Phys. Rev. A **21**, 293 (1980).
[48]R. C. Davidson and H. S. Uhm, Phys. Fluids **23**, 2076 (1980).
[49]H. P. Freund and P. Sprangle, Phys. Rev. A **28**, 1835 (1983).
[50]P. Sprangle, C. M. Tang, and I. Bernstein, Phys. Rev. A **28**, 2300 (1983).
[51]R. C. Davidson and J. S. Wurtele, IEEE Trans. Plasma Sci. **PS-13**, 464 (1985).
[52]R. C. Davidson, Phys. Fluids **29**, 267 (1986).
[53]M. V. Goldman, Phys. Fluids **13**, 1281 (1970).
[54]R. C. Davidson, *Methods in Nonlinear Plasma Theory* (Academic, New York, 1972), Chap. 4.